

## Gold Supported on Strontium Surface-Enriched $\text{CoFe}_2\text{O}_4$ Nanoparticles: a Strategy for the Selective Oxidation of Benzyl Alcohol

Laise N. S. Pereira,<sup>a</sup> Carlos E. S. Ribeiro,<sup>a</sup> Aryane Tofanello,<sup>b</sup> Jean C. S. Costa,<sup>a</sup> Carla V. R. de Moura,<sup>b</sup> Marco A. S. Garcia<sup>a</sup> and Edmilson M. de Moura<sup>b</sup> \*<sup>a</sup>

<sup>a</sup>Departamento de Química, Universidade Federal do Piauí, 64049-550 Teresina-PI, Brazil

<sup>b</sup>Centro de Ciências Naturais e Humanas, Universidade Federal do ABC, 09210-580 Santo André-SP, Brazil

The synthesis of efficient and reusable gold-based catalysts for the selective oxidation of alcohols is a strategy for the development of green processes. Pre-formed nanoparticles syntheses are an easy way to produce controlled-nanosized gold materials; however, the selection of a support is not trivial. Herein, we proposed a  $\text{CoFe}_2\text{O}_4$  support enriched with  $\text{Sr}(\text{OH})_2$ , which holds remarkable properties and is suitable for the synthesis of a stable gold-based catalyst for the oxidation of benzyl alcohol. We suggested that the interaction between the  $\text{CoFe}_2\text{O}_4$  and the  $\text{Sr}(\text{OH})_2$  is highly important for the performance of the catalyst. Under the base-free condition of 2.5 h, 100 °C and 2 bar of  $\text{O}_2$ , the catalyst reached 58% of conversion with 76% of selectivity to benzaldehyde. With  $\text{K}_2\text{CO}_3$  addition, the conversion and selectivity to benzaldehyde increased to 87% and 88%, respectively. Any gold leaching was detected in 5 successive runs, attesting the noticeable stability that the catalyst presents. This work provides great potential for the selective oxidation of alcohols with high activity since the magnetic properties of the catalyst provide an easy route and allows the separation of the medium reaction. In addition, we are here proposing an important interaction between the  $\text{Sr}(\text{OH})_2$  and the magnetic nanoparticles.

**Keywords:** cobalt ferrite, strontium hydroxide, oxidation, enrichment, supported catalyst

### Introduction

Selective oxidation of alcohols is one of the most significant transformations of organic chemistry since it is essential for industrial intermediates production, such as ketones, epoxides, aldehydes and acids.<sup>1-4</sup> In order to avoid the use of stoichiometric toxic oxidants, metal catalysts have been proposed as green alternatives since they enable the use of molecular oxygen in the gas phase, which generates only water as a byproduct.<sup>5-8</sup> Prati *et al.*<sup>9,10</sup> and Porta *et al.*<sup>11</sup> have shown that gold-based catalysts can be effective for the oxidation of alcohols with increased selectivity when compared to platinum and palladium catalysts;<sup>12</sup> however, the application of such materials is not observed in large-scale production. Thus, attempts to reach this goal involve deep knowledge of the oxidation process itself. In this scenario, the understanding of the oxidation of a specific simple substrate can contribute to further applications of more complex substrates. Benzyl alcohol oxidation is a much-known reaction, yet very

used as a model molecule since it can be used to evaluate new systems. In addition, such a model reaction can bring insights related to activity and selectivity for partial oxidation of a given process.

On the other hand, the synthesis of stable catalysts is just as, if not more, important as the oxidation reaction pathway familiarity. In this aspect, the nanotechnology can support in the efficiency of these catalysts by using metal nanoparticles (MNPs) onto inorganic supports via immobilization under different conditions.<sup>6,13-15</sup> Although syntheses of heterogeneous catalysts are very explored in the literature, direct efforts towards the comprehension of the nature of supports are increasing since the metal-support interactions mechanisms have not been fully elucidated.

Among all sort of supports that can be used for the MNPs impregnation processes, alkaline earth oxides and hydroxides can play an important role in oxidation reactions. The reason for that is the intrinsic basicity<sup>16</sup> that such materials present, which would help the substrate-activation process by the abstraction of the hydrogen of the alcohol as it is considered essential for the reaction beginning.<sup>17</sup> Temperature-programmed desorption measurements of

\*e-mail: mmoura@ufpi.edu.br

alkaline earth metal oxides, performed under the same conditions, showed the following decreasing trend for the strength of basic sites: BaO > SrO > CaO > MgO.<sup>18</sup> Some reports have been exploring MgO,<sup>19,20</sup> CaO<sup>21</sup> and Mg(OH)<sub>2</sub><sup>22</sup> as support for gold catalysts. Although BaO is toxic and environmentally hostile, SrO would be a good candidate as support for Au nanoparticles (NPs) for oxidation reactions. Also, other strontium-based compounds are neglected and not fully considered in the literature, as the Sr(OH)<sub>2</sub>. Addition of base may be required for oxidation reactions, although the basicity of the carrier can also have a significant effect.<sup>23</sup>

While the support choice is somehow difficult due to its importance in a given catalytic system, the separation and recyclability of catalysts are challenging. Thus, the immobilization of catalysts on magnetic materials has been a trend in the catalysis field as an attractive alternative for better handling MNPs.<sup>24</sup> The literature highlights the use of such magnetic materials in the fabrication of nanocatalysts as an important tool for easy separation and recovery from the reaction medium upon application of an external magnetic field.<sup>25</sup> However, the use of nanoscale magnetic NPs can improve the dispersion of the amorphous supports prior to the MNPs immobilization, which undoubtedly improves the catalytic activity of the catalyst.<sup>26</sup>

Previously, we reported the preparation of a catalyst through the immobilization of Au NPs on Sr(OH)<sub>2</sub>, which enabled the catalyst activity for the oxidation of benzyl alcohol without base addition. Herein, we explored the enrichment of CoFe<sub>2</sub>O<sub>4</sub> NPs with strontium hydroxide and its subsequent impregnation with gold as a strategy for the preparation of an oxidation catalyst with high activity and selectivity. The novelty of this work is the impregnation of Sr(OH)<sub>2</sub> on the MNPs, which enabled an improvement on the catalyst performance when compared to a simple system comprised only of Sr(OH)<sub>2</sub> and Au NPs. In addition, we brought some insights on the role of the MNPs on the catalysis, which is not very discussed in the literature. Also, the structural characterization and stability were evaluated and a full characterization of the material was investigated in details.

## Experimental

### Preparation of CoFe<sub>2</sub>O<sub>4</sub>

Cobalt ferrite NPs were synthesized using a co-precipitation method<sup>27</sup> with modifications, replacing Fe<sup>2+</sup> by Co<sup>2+</sup>. In a standard process, 2.5 mL of an aqueous 2 mol L<sup>-1</sup> HCl solution of CoCl<sub>2</sub>·6H<sub>2</sub>O (4.1 mmol) was mixed with 5 mL of an aqueous solution of FeCl<sub>3</sub>·6H<sub>2</sub>O (8.2 mmol). The final solution was poured off into 125 mL of an aqueous

ammonium hydroxide solution (0.7 mol L<sup>-1</sup>) under stirring (900 rpm, Arec X, Velp Scientifica) with a black precipitate formation. After stirring for 2 h, the product was separated with a neodymium magnet (Nd<sub>2</sub>Fe<sub>14</sub>B) and the supernatant was collected. The black precipitate was washed three times with hot distilled water (200 mL, 80 °C) and once with acetone (100 mL) before being placed in an oven at 80 °C. At that time, the material was placed in a muffle furnace in air at 800 °C for 3 h, at a heating rate of 10 °C min<sup>-1</sup>.

### Strontium oxide preparation

The procedure for the strontium oxide preparation was carried out following the method described by Ke *et al.*<sup>28</sup> Basically, SrCO<sub>3</sub> was calcined at 1100 °C for 5 h in a muffle furnace in an air atmosphere. The compound was shortly used after its synthesis.

### Support preparation

The CoFe<sub>2</sub>O<sub>4</sub> enrichment with the strontium oxide was performed using an impregnation method.<sup>20</sup> Both materials were mixed in acetone under stirring (1000 rpm) considering a mass ratio of 1:5. The process was maintained for 24 h. After this time, the material was dried in an oven at 100 °C for 12 h.

### Catalyst preparation

The catalyst was prepared using a sol-immobilization method with modifications.<sup>29</sup> The original procedure was performed for a bimetallic system and here only gold was used as active species. In a typical procedure, 1.80 mL of a 2.0 wt.% aqueous solution of polyvinyl alcohol (PVA 80%, 36 mg) was added to an acetonic solution of HAuCl<sub>4</sub> (172.5 mg, 300 mL) under magnetic stirring (900 rpm). After this step, a freshly prepared 7.65 mL of NaBH<sub>4</sub> aqueous solution (0.1 mol L<sup>-1</sup>, prepared in ice-cold water) was added to reduce the metal, maintaining the magnetic stirring. The solution turned dark instantly and the stirring was continued for an additional 30 min. After this time, the support was added (1.5 g) to the solution and stirred at room temperature for 3 h. The catalyst was separated using a neodymium magnet and washed three times with hot water (200 mL, 80 °C) and once with acetone (100 mL) before being placed in an oven at 80 °C for 12 h.

### Catalytic reactions

The reactions were carried out in a Fischer-Porter glass reactor with a capacity of 100 mL at 2 bar of O<sub>2</sub> and 100 °C,

except when mentioned. At the Fischer-Porter reactor, the catalyst (4.1 mmol of Au) and benzyl alcohol (9.6 mmol) were added using magnetic stirring. Typically, the reaction was performed for 2.5 h, although some modifications were also explored. When the reaction stopped, the catalyst was separated from the reaction medium using the neodymium magnet simply placing it on the reactor glass wall. For analytical analyses, 5  $\mu\text{L}$  of the final solution were collected and added to 1 mL of  $\text{CH}_2\text{Cl}_2$ . The injection in the gas chromatograph was performed using 1  $\mu\text{L}$  of the solution. The conversion of benzyl alcohol, product selectivity and carbon mass balance were calculated as follows:

$$\text{Conversion (\%)} = \frac{\text{moles of the substrate reacted}}{\text{initial moles of substrate}} \times 100 \quad (1)$$

$$\text{Selectivity (\%)} = \frac{\text{moles of product of interest}}{\text{moles of all the products}} \times 100 \quad (2)$$

$$\text{Carbon mass balance (\%)} = \frac{\text{total moles of products and unreacted substrate}}{\text{initial moles of the substrate}} \times 100 \quad (3)$$

For the recycling experiments using  $\text{K}_2\text{CO}_3$ , the catalyst was washed three times with water to remove the previously added base from the former run, and then three times with acetone.

### Characterizations

X-ray diffraction (XRD) analyses were carried out using Bruker D8 Advance equipment (Bruker AXS GmbH, Karlsruhe, Germany) with  $\text{Cu K}\alpha$  radiation ( $\lambda = 1.54056 \text{ \AA}$ ) and a graphite monochromator. The filament current was 40 mA and the voltage of the copper emission tube was 40 kV, with a range from 10 to  $90^\circ$  with a  $0.02^\circ$  step size (the chosen measuring time was 5 s *per* step). Surface parameters were determined by Brunauer-Emmett-Teller (BET) method in a relative pressure range of  $0.07 < P/P_0 < 0.3$ ; Barrett, Joyner and Halenda (BJH) method was used to determining the average pore diameter. Gas chromatography (GC) analyses were performed using Shimadzu 2010 chromatograph equipped with flame ionization detector (FID) and Carbowax capillary column, using *p*-xylene as standard. The magnetic measurements (M-H curve) were carried out at room temperature with the help of an MPMS3-SQUID magnetometer (Quantum Design) with a magnetic field cycled between  $-22$  and  $+22$  kOe. Transmission electron microscopy (TEM) images were obtained using JEOL JEM 2100 (operating at 110 kV) microscope. The nanoparticles' size was determined by using an open source image processing program ImageJ.<sup>30</sup>

For that, 350 particles were considered. Leaching analyses were performed using inductively coupled plasma-atomic emission spectrometry (ICP OES, Spectro brand, Arcos model). The X-ray photoemission spectra were obtained with a Scienta Omicron ESCA + spectrometer system equipped with an EA 125 hemispherical analyzer and an XM 1000 monochromated X-ray source in  $\text{Al K}\alpha$  (1486.7 eV). The analyses were performed by using CasaXPS processing software.<sup>31</sup> The phase composition was determined by Rietveld refinement using ReX software.<sup>32</sup>

## Results and Discussion

Recently, we have reported the synthesis of highly dispersed Au NPs on a magnetic material comprised of  $\text{CoFe}_2\text{O}_4$  enriched with  $\text{MgO}$  or  $\text{Mg}(\text{OH})_2$ .<sup>26</sup> The Au catalyst presented good performances in the presence of  $\text{K}_2\text{CO}_3$ , without significant loss of activity up to 5 runs. A non-magnetic catalyst was also proposed by our group;<sup>23</sup> however, using  $\text{Sr}(\text{OH})_2$  as support. Such gold-based catalyst presented lower activity and selectivity when compared to the former, but was recyclable and showed an intrinsic basicity that enabled its application with and without external base addition with good results. Both materials presented the important feature of not presenting leaching of metal to the reaction medium, which is highly important to the synthesis of heterogeneous catalysts. Herein, we decided to link both projects, i.e., to use  $\text{CoFe}_2\text{O}_4$  magnetic NPs with a strontium enrichment. Subsequently, PVA-stabilized Au NPs were immobilized over the support using a sol-impregnation method in an acetonic medium, in order to try to maintain the SrO prepared by the calcination of the  $\text{SrCO}_3$ . It is worthy to mention that the immobilization on  $\text{CoFe}_2\text{O}_4$  NPs was just possible with the enrichment.

The procedure for the strontium compound obtainment was different from the previously reported; in addition, it had to undergo a process to efficiently prepare  $\text{CoFe}_2\text{O}_4$  magnetic NPs enriched with such material. Thus, the phase composition of the prepared substance had to be characterized by Rietveld refinement in order to specifically quantify the number and amount of crystalline phases on the modified magnetic material. Figure 1 shows the refined pattern of the material; the diffraction pattern indexed three crystalline phases:  $\text{CoFe}_2\text{O}_4$  (ICSD 109045),  $\text{Sr}(\text{OH})_2$  (ICSD 15167) and  $\text{Sr}(\text{OH})_2 \cdot \text{H}_2\text{O}$  (ICSD 63016). The XRD pattern indexing each peak was also presented (Figure S1, Supplementary Information (SI) section); discernible peaks can be indexed to (220), (311), (400), (422), (511) and (440) planes of a cubic structure  $\text{CoFe}_2\text{O}_4$ , in agreement with the standard data of  $\text{CoFe}_2\text{O}_4$  (JCPDS

No. 79-1744). The major phase was comprised of Sr(OH)<sub>2</sub> (53%), with remained phases comprised of Sr(OH)<sub>2</sub>·H<sub>2</sub>O (32%) and cubic CoFe<sub>2</sub>O<sub>4</sub> (15%). The indexed peaks allowed the proposition of the unitary cell (Figure S2, SI section) of each phase and their specific parameters (Table S1, SI section). The results unambiguously showed that the impregnation in the acetonic medium was not able to maintain the SrO phase, corroborating with our previous studies.<sup>19</sup> The catalyst was designated as Au/Sr(OH)<sub>2</sub>/CoFe<sub>2</sub>O<sub>4</sub> as the correct strontium phases were elucidated by the refinement.

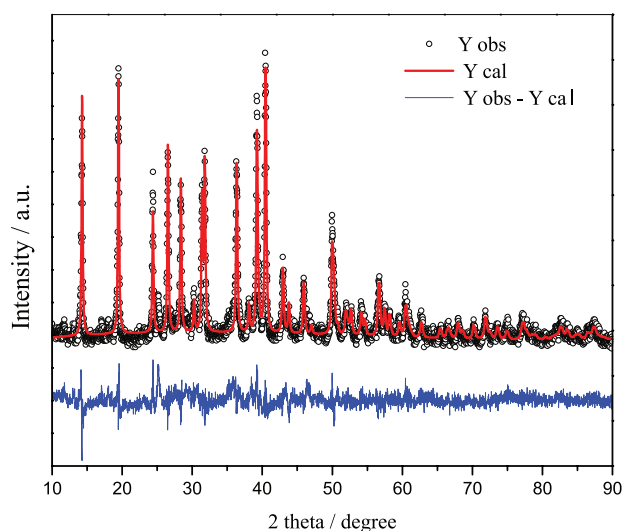


**Figure 1.** Rietveld refinement plot for Au/Sr(OH)<sub>2</sub>/CoFe<sub>2</sub>O<sub>4</sub> catalyst showing the observed, calculated and difference between X-ray patterns.

The as-prepared Au/Sr(OH)<sub>2</sub>/CoFe<sub>2</sub>O<sub>4</sub> catalyst presented 2.0 wt.% Au as evidenced by ICP OES analysis. Such sample was characterized by TEM and Figure 2a shows well-dispersed Au NPs onto the support, i.e., the Sr(OH)<sub>2</sub>-enriched CoFe<sub>2</sub>O<sub>4</sub> NPs were indeed an efficient candidate for the studies here described since uniform

MNPs coverage is essential for heterogeneous catalysis.<sup>6</sup> The pre-formed PVA-stabilized Au NPs synthesis was able to lead the preparation of a catalyst with narrow size distribution, as showed by the histogram displayed in Figure 2b, which presented particles size around 6.1 ± 1.9 nm. Since the procedure did not mean to prepare core-shell structures, magnetic properties are important to suggest effectiveness on the interaction of the CoFe<sub>2</sub>O<sub>4</sub> NPs and the Sr(OH)<sub>2</sub> prepared.

The magnetic properties of the bare CoFe<sub>2</sub>O<sub>4</sub> and the Sr(OH)<sub>2</sub>/CoFe<sub>2</sub>O<sub>4</sub> NPs were investigated by measuring magnetizations as a function of an external magnetic field at 298 K. Figure 3a shows the magnetic hysteresis loops of the samples; the M-H curves were analyzed to extract some magnetic information, such as the saturation magnetization (MS), remanence (MR) and coercivity (Hc). It is possible to observe the same profile of the hysteresis curve, i.e., the same response to the magnetic field application for the two analyzed catalysts. At room temperature, both curves exhibited ferromagnetic behavior with no anomalous shape associated with mixtures of isostructural phases, consistent with the presence of a unique spinel cubic phase.<sup>33,34</sup> For clarity, a zoomed view at low magnetic fields is displayed in the inset of Figure 3a for the Sr(OH)<sub>2</sub>/CoFe<sub>2</sub>O<sub>4</sub> NPs. The hysteresis loop for the CoFe<sub>2</sub>O<sub>4</sub> is characterized by a coercive field of 1.5 kOe and the value five times smaller for the Sr(OH)<sub>2</sub>/CoFe<sub>2</sub>O<sub>4</sub> NPs is due to the presence of SrO coating on the ferrite. The MS for the CoFe<sub>2</sub>O<sub>4</sub> is about 81.6 emu g<sup>-1</sup>, in agreement with the reported data for the bulk sample.<sup>35</sup> Although the saturation magnetization for Sr(OH)<sub>2</sub>/CoFe<sub>2</sub>O<sub>4</sub> is smaller than the value observed for the CoFe<sub>2</sub>O<sub>4</sub>, the coated catalyst may be efficiently separated from the reaction medium upon magnetization with a permanent magnet, as observed in the recycling experiments, which will be discussed below. The magnetization as a function of temperature under

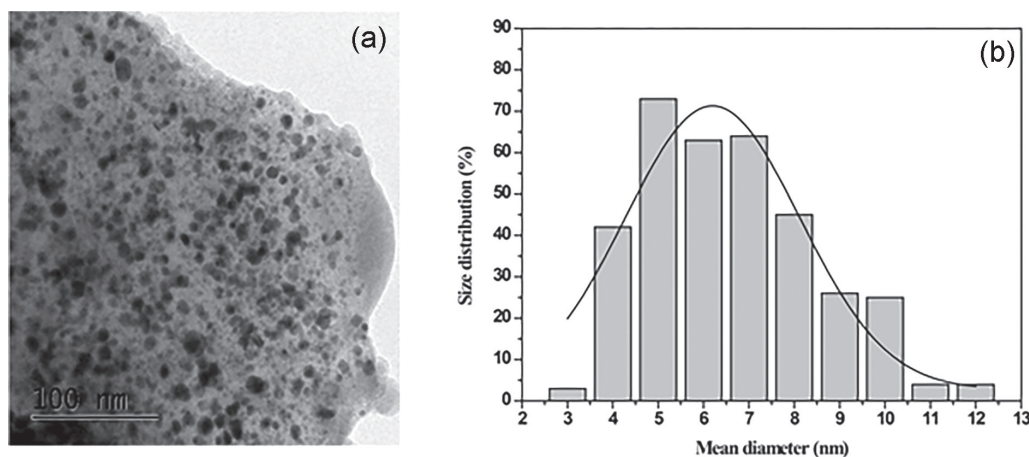


**Figure 2.** (a) TEM image of Au/Sr(OH)<sub>2</sub>/CoFe<sub>2</sub>O<sub>4</sub> catalyst and (b) respective size distribution histogram.

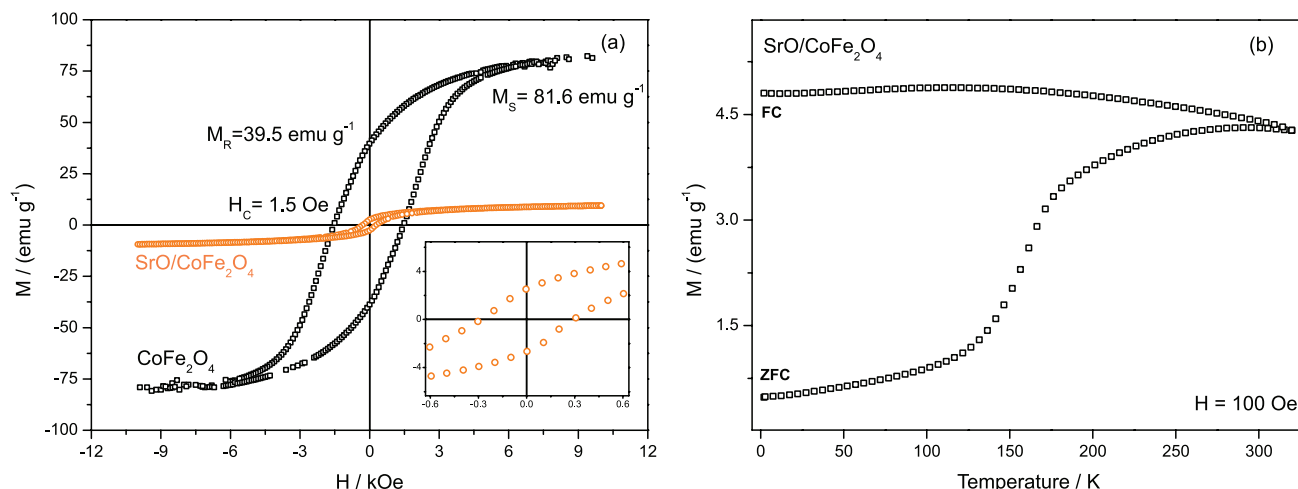


**Figure 3.** Magnetization curves for  $\text{CoFe}_2\text{O}_4$  (black dots) and  $\text{Sr}(\text{OH})_2/\text{CoFe}_2\text{O}_4$  (orange dots) NPs: SQUID measurements of (a) magnetization hysteresis curves; (b) field-cooled (FC) and zero-field-cooled (ZFC) curves for  $\text{Sr}(\text{OH})_2/\text{CoFe}_2\text{O}_4$  NPs.

zero-field cooled (ZFC) and field-cooled (FC) regimes is shown in Figure 3b.

The ZFC curve indicates that the magnetization values increase with temperature, as shown in Figure 3a, in contrast to the profile of the FC curve. The blocking temperature of  $\text{Sr}(\text{OH})_2/\text{CoFe}_2\text{O}_4$  was 290 K. The material has the advantage of being recovered by a protective layer and maintain its magnetic properties. At room temperature, the  $\text{Sr}(\text{OH})_2$ -enriched  $\text{CoFe}_2\text{O}_4$  exhibited lower hysteresis compared to bare NPs. Therefore, the separation of the catalyst using a magnet will be more effective in the bare  $\text{CoFe}_2\text{O}_4$  NPs, which does not prevent the separation of the  $\text{Sr}(\text{OH})_2/\text{CoFe}_2\text{O}_4$  NPs, making them a suitable support for the gold catalyst, as expected. Further catalytic results presented herein will demonstrate the increased performance of the catalyst, which helps to reinforce that the interaction of  $\text{CoFe}_2\text{O}_4$  NPs and the  $\text{Sr}(\text{OH})_2$  was efficient.

Literature has shown that  $\text{Au}^0$  NPs onto different supports have presented remarkable activity on oxidation reactions.<sup>27,28</sup> Thus, with a focus on Au chemical states, XPS analysis was performed. Figure 4 presents the spectra for Au 4f. As expected due to the pre-formed NPs preparation procedure used, the XPS spectrum of the Au 4f peaks displays two indicative peaks of metallic Au at binding energies of 82.75 and 86.45 eV, in Au 4f<sub>7/2</sub> and Au 4f<sub>5/2</sub> states, which characterizes the reduction of  $\text{Au}^{3+}$  ions by  $\text{NaBH}_4$ .<sup>29</sup>

To investigate the performance of the catalyst, the as-prepared material was applied in the oxidation reaction of benzyl alcohol. All the experiments were carried out under  $\text{O}_2$  atmosphere. The compounds benzyl alcohol, benzaldehyde and benzyl benzoate are the major components of all the reaction mixtures with a carbon

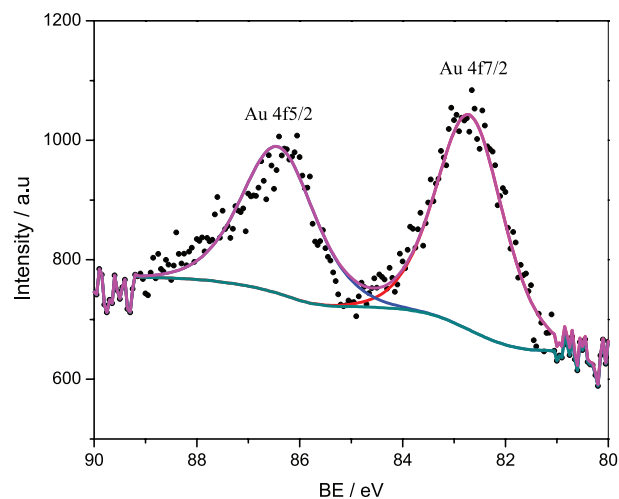
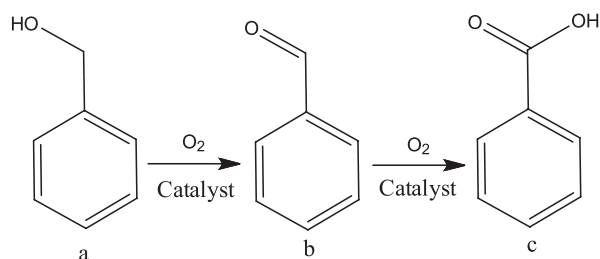


**Figure 4.** XPS spectra of sample  $\text{Au}/\text{Sr}(\text{OH})_2/\text{CoFe}_2\text{O}_4$ .

mass balance > 95%. Scheme 1 presents the main products observed for the model reaction. When benzyl benzoate was obtained, it was mentioned straightforward in the text. A blank test with only the substrate, without catalyst or base, was performed and presented just 1% of conversion, without any control of selectivity (34% of benzaldehyde, 24% of benzyl benzoate and 42% of benzoic acid). Additional control experiments employing the separate components of the support, as well as the magnetic-enriched support itself (Table 1, entries 1, 2 and 3), were performed. The three analyses showed no reaction under standard conditions: 100 °C, 2 bar of  $\text{O}_2$  and 2.5 h. However, when just  $\text{Au}/\text{Sr}(\text{OH})_2$  was used as the catalyst, 7% of conversion was achieved, with 42% of selectivity for benzaldehyde, 49% for benzyl benzoate and 9% for benzoic acid. Employing the same reaction conditions, the catalyst  $\text{Au}/\text{Sr}(\text{OH})_2/\text{CoFe}_2\text{O}_4$  without base addition was also studied.



**Scheme 1.** Schematic representation of the benzyl alcohol oxidation reaction, which shows only the products obtained in the studies here presented: (a) benzyl alcohol; (b) benzaldehyde and (c) benzoic acid.

Interestingly, a conversion of 58% was achieved, with 75% selectivity for benzaldehyde (Table 1, entry 2), with no benzyl benzoate formation. Herein, it is possible to highlight the effect of the interaction between the Sr(OH)<sub>2</sub> and the CoFe<sub>2</sub>O<sub>4</sub> NPs, once the performance of the catalyst remarkably improved. The results are inspiring since magnesium-based catalysts, under similar base-free conditions, presented much lower performances.<sup>19,20</sup> Such improvements cannot be associated only with surface characteristics because, after the gold impregnation, the surface area and pore volume were found to considerably decrease (Table S2 and Figure S3, SI section). However, this remarkable result is very significant since it sustains our suggestion on the importance of the CoFe<sub>2</sub>O<sub>4</sub> NPs enrichment with Sr(OH)<sub>2</sub>.

**Table 1.** Oxidation reactions of benzyl alcohol under base-free conditions<sup>a</sup>

entry	Catalyst	Conversion / %	Selectivity / %	
			Benzaldehyde	Benzoic acid
1	CoFe <sub>2</sub> O <sub>4</sub>	0	–	–
2	Sr(OH) <sub>2</sub>	0	–	–
3	Sr(OH) <sub>2</sub> /CoFe <sub>2</sub> O <sub>4</sub>	0	–	–
4	Au/Sr(OH) <sub>2</sub> <sup>b</sup>	7	42	9
5	Au/Sr(OH) <sub>2</sub> /CoFe <sub>2</sub> O <sub>4</sub>	58	75	25

<sup>a</sup>Reaction conditions (solventless): 9.6 mmol of benzyl alcohol, 4.1 mmol of Au (catalyst), 2 bar of O<sub>2</sub>, reaction temperature 100 °C, 2.5 h; carbon mass balance > 95%; <sup>b</sup>49% of benzyl benzoate was also obtained.

Catalytic properties can be optimized by modulation of composition, structure, shape, and size of materials;<sup>34</sup> however, the strontium material was synthesized under non-controlled conditions, which hampered its application. The electrostatic interaction<sup>35</sup> of the Sr(OH)<sub>2</sub> with the CoFe<sub>2</sub>O<sub>4</sub> can improve the dispersion of the former and increase its available surface, due to geometric and electronic issues.<sup>25</sup> The higher homogeneity of the support provides enhancements on the metal-support interactions. This suggestion can be supported by XPS composition analysis (Figure S4, SI section). The Au atomic concentration

(2.90%) was higher than the previous data obtained for the gold catalyst support on Sr(OH)<sub>2</sub> without the CoFe<sub>2</sub>O<sub>4</sub> NPs (0.13 at.% Au).<sup>23</sup> Such a result certainly improves the catalytic performance once the metal availability is higher.

In addition, the interaction of the materials may explain the augmentation in the performance of the catalyst as the surface energy of the support may be different from the Sr(OH)<sub>2</sub> itself. Gao *et al.*<sup>36</sup> performed theoretical studies that revealed that adsorption energies decreased in the presence of an external magnetic field, increasing the catalytic activity of Pd NPs supported on Co<sub>3</sub>[Co(CN)<sub>6</sub>]<sub>2</sub> NPs for Suzuki cross-coupling reactions. For the Au/Sr(OH)<sub>2</sub>/CoFe<sub>2</sub>O<sub>4</sub> catalyst, the magnetic field provided by the ferrite can be considered an important tool that influences the structure and properties of materials.<sup>37,38</sup> With the proposed arrangement in this work (Au/Sr(OH)<sub>2</sub>/CoFe<sub>2</sub>O<sub>4</sub>), the catalyst acts as a binding support in which the Au NPs are deposited, and the synergistic interactions between the gold and the Sr<sup>2+</sup> have a key role in achieving high activity.<sup>39</sup> In addition to the results herein presented, Nepal and Srinivas<sup>39</sup> have proposed that the reaction happens in the interface between the Au NPs and titanate-modified nanotubes with basic alkali and alkaline earth metal ions, which is highly related to the support basicity. We propose, based on such studies, that the reaction also happens on the metal-support interface; which requires similar long-range interaction between the metal and the modified support to be plausible.

Experiments were performed by varying temperature and pressure (Table 2) in an attempt to improve the catalytic performance of the catalyst. One may notice that the temperature increasing from 100 to 160 °C (Table 2, entries 6-9) was not able to considerably increase the activity of the catalyst, although some improvement was obtained in the selectivity of benzaldehyde, suggesting that the partially oxidized product is thermodynamically controlled. Thus, maintaining the temperature (100 °C), the pressure changing was analyzed, from 1 to 4 bar of O<sub>2</sub>, since the glass reactor does not hold much higher pressures. Clearly, the pressure effect is higher than the observed for the temperature augmentation; however, over 2 bar of O<sub>2</sub>, there is no significant change in the selectivity and the activity is barely changed (Table 2, entries 10-12). When K<sub>2</sub>CO<sub>3</sub> was added to the reaction medium, not only the activity increased, but also the selectivity for benzaldehyde (Table 2, entry 13). Such enhancement was expected as the presence of a base is considered by the literature important for the substrate hydrogen abstraction.<sup>17</sup>

Once again, such a result presents a significant improvement when compared to the catalyst without the CoFe<sub>2</sub>O<sub>4</sub> NPs enrichment, using only Sr(OH)<sub>2</sub> as support,

previously published. In addition, our previous study showed the base presence was important for the catalyst stability.<sup>23</sup> In addition, we have performed experiments using commercial materials in a non-nanoscale size ( $\text{Al}_2\text{O}_3$ ,  $\text{SiO}_2$ ,  $\text{TiO}_2$ ), as the  $\text{Sr}(\text{OH})_2$  material used herein. The best performance using the same conditions employed herein was for the  $\text{Au}/\text{Al}_2\text{O}_3$  catalyst; not just the conversion was lower (76%), but the selectivity for the partially oxidized product was just 22%.<sup>6</sup> The data obtained with the  $\text{Au}/\text{Sr}(\text{OH})_2/\text{CoFe}_2\text{O}_4$  material corroborates the importance of the  $\text{CoFe}_2\text{O}_4$  enrichment process.

Based on the literature that deals with the oxidation of benzyl alcohol, it is noteworthy that the partially oxidized product is highly desirable. Although under different reaction conditions, articles (Table 3) presented lower conversions when compared even with our base-free catalyst application conditions, with comparable selectivity for benzaldehyde,<sup>38,40</sup> except when a zirconium-based material was used as support.<sup>41</sup> Thus, the novel catalyst proposed is able to accomplish the required conditions to be used for the oxidation of alcohols.

To fulfill its characterizations, the conversion *vs.* time profile of the reaction performed with the  $\text{Au}/\text{Sr}(\text{OH})_2/\text{CoFe}_2\text{O}_4$  catalyst in presence of  $\text{K}_2\text{CO}_3$  is presented in Figure 5. The benzyl alcohol oxidation was examined over for 24 h. The conversion increasing was more pronounced in the first 2.5 h of reaction and became moderate up to 24 h. Thus, to further analyze the stability of the herein reported catalyst, 2.5 h would be enough for the recyclable experiments. One may notice that there is no remarkable change in the selectivity up to the end of the analysis.

Also, our catalyst exhibited high activity and good recyclability, since the conversion decreased slightly even after the execution of 5 successive cycles; after each reaction, upon application of an external magnet, the catalyst was separated from the reaction medium, washed with water to remove the base and with  $\text{CH}_2\text{Cl}_2$  before drying. Then, the same base quantity was added and a new reaction was carried out. The recycle experiments were performed with  $\text{K}_2\text{CO}_3$  addition since without the base, gold leaching was observed. In 2.5 h, under 100 °C and 2 bar of  $\text{O}_2$ , the catalyst was very stable in 5 runs (Figure 6), without

**Table 2.** Oxidation reactions of benzyl alcohol without base addition using  $\text{Au}/\text{Sr}(\text{OH})_2/\text{CoFe}_2\text{O}_4$  catalyst

entry <sup>a</sup>	Pressure / bar	Temperature / °C	Conversion / %	Selectivity / %	
				Benzaldehyde	Benzoic acid
6	2	100	58	75	25
7	2	120	59	77	23
8	2	140	63	78	22
9	2	160	66	80	20
10	1	100	36	42	58
11	3	100	63	78	22
12	4	100	64	78	22
13 <sup>b</sup>	2	100	87	88	12

<sup>a</sup>Reaction conditions (solventless): 9.6 mmol of benzyl alcohol, 4.1 mmol of Au (catalyst), 2.5 h; <sup>b</sup>addition of 0.33 mmol of  $\text{K}_2\text{CO}_3$ . Carbon mass balance > 95%.

**Table 3.** Comparison of catalytic conditions of the proposed method with some methods of the literature

Catalyst	Conversion / %	Selectivity / %		Reference
		Benzaldehyde	Benzoic acid	
$\text{Au}/\text{Sr}(\text{OH})_2/\text{CoFe}_2\text{O}_4^{\text{a,b}}$	58.3	75.4	24.6	this work
$\text{Au}/\text{Sr}(\text{OH})_2/\text{CoFe}_2\text{O}_4^{\text{a,c}}$	87.4	88.1	11.9	this work
$\text{Au}/\text{Mn}-\text{CeO}_2^{\text{d}}$	43.22	> 99	–	38
$\text{Au}/\text{MnO}_2^{\text{e}}$	12.2	87.7	12.3	40
$\text{Au}/\text{UiO}-66^{\text{f,g}}$	53.8	53.7	not mentioned	42

<sup>a</sup>Reaction conditions (solventless): 9.6 mmol of benzyl alcohol, 4.1 mmol of Au (catalyst), 2 bar of  $\text{O}_2$ , reaction temperature 100 °C, 2.5 h; <sup>b</sup>free base addition; <sup>c</sup>with 0.33 mmol of base  $\text{K}_2\text{CO}_3$ ; <sup>d</sup>reaction conditions: toluene as solvent, 4 mL; benzyl alcohol, 4 mmol; catalyst, 100 mg; 3.5 wt.% Au;  $\text{O}_2$ , 50 mL  $\text{min}^{-1}$ ; reaction time, 3 h; 90 °C; dodecane as an internal standard; <sup>e</sup>reaction conditions: 0.1 g catalyst, 10 mmol benzyl alcohol, 80 °C, 5 h, 5 mL  $\text{min}^{-1}$   $\text{O}_2$ ; <sup>f</sup>reaction conditions: benzyl alcohol, 10 mL; catalyst, 50 mg;  $\text{K}_2\text{CO}_3$ , 0.6 g;  $\text{H}_2\text{O}$ , 0.05 mL;  $\text{O}_2$  at 0.004  $\text{m}^3 \text{h}^{-1}$ , 80 °C, 10 h; <sup>g</sup>zirconium-based metal-organic framework. Carbon mass balance > 95%.

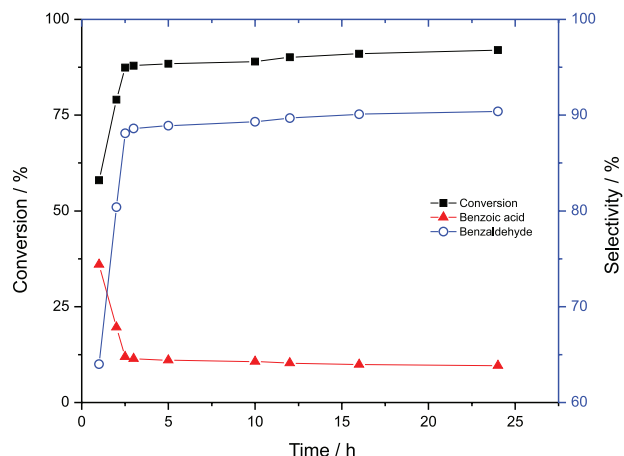


**Figure 5.** Influence of the reaction time on the conversion and selectivity in the oxidation of benzyl alcohol over  $\text{Au/Sr(OH)}_2/\text{CoFe}_2\text{O}_4$  catalyst.

loss of activity and selectivity, with potential for more uses. ICP OES analyses were performed and showed no leaching of gold was detected after 5 catalytic cycles. Such results indicate that the presence of the magnetic support was able to stabilize the catalytic Au NPs, preventing their aggregation and leaching. Thus, the system can be considered as a catalyst with high activity and good reuse capacity after magnetic separation. Clearly, the material is stable and may be applicable to the oxidation of more complex substrates.

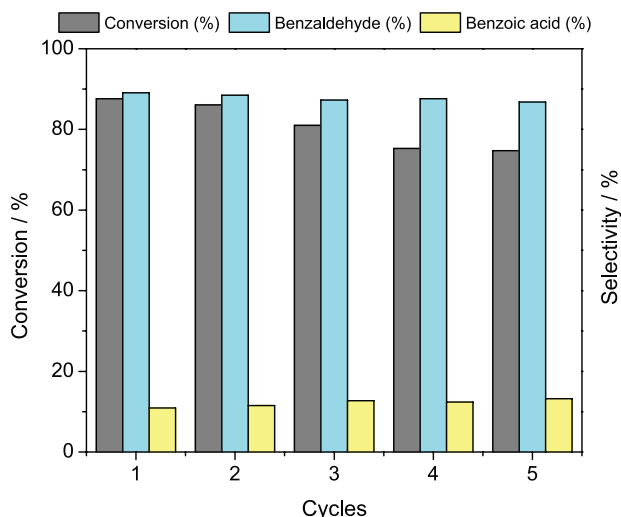


**Figure 6.** Recycling tests for the  $\text{Au/Sr(OH)}_2/\text{CoFe}_2\text{O}_4$  catalyst.

## Conclusions

We presented herein the synthesis of a heterogeneous catalyst comprised of Au NPs supported on a  $\text{Sr(OH)}_2$ -enriched  $\text{CoFe}_2\text{O}_4$  support, with a controlled size of metal NPs and well dispersion over the support. Rietveld refinement and XPS gave us data that supports a

good characterization of the catalyst regarding its specific chemical content. The catalyst exhibited remarkable and efficient activity for the benzyl alcohol oxidation. The intrinsic basicity that  $\text{Sr(OH)}_2$  holds allowed the employment of the catalyst with or without  $\text{K}_2\text{CO}_3$  adding in the presence of the magnetic NPs. The catalyst could be recovered by an external magnet and successively reused five cycles without significant loss of activity with an almost complete conversion. The enrichment of the magnetic NPs was essential for the gold impregnation since before such modification no metal loading was possible. In addition to the high magnetization the support covers, we suggested that the interaction between the strontium material with the magnetic NPs was decisive for the catalytic performance, not just for the conversion obtained, but also for the selectivity for the partially oxidized product. XPS analyses helped to bring insights on this matter. Regarding the performance of the catalyst, an activity close to 60% was obtained in base-free conditions and in 2.5 h, but the  $\text{K}_2\text{CO}_3$  addition significantly improved the activity of the catalyst (87%), moderately increasing the selectivity. Such performance was reasonably an enhancement considering our previous studies.

## Supplementary Information

Supplementary data with X-ray powder diffraction patterns, parameters obtained from the Rietveld refinery, unit cells, chemical analysis and surface properties,  $\text{N}_2$  adsorption/desorption isotherms and XPS pattern of  $\text{Au/Sr(OH)}_2$  catalyst/ $\text{CoFe}_2\text{O}_4$ , are available at <http://jbcs.sbq.org.br> as PDF file.

## Acknowledgments

The authors acknowledge financial support from FAPESP, CAPES and CNPq and the technical support of the Center for Strategic Technology of the Northeast (CETENE-PE). Thanks to CCMC/CDMF (FAPESP No. 2013/07296-2, Brazil) and CEM-UFABC (Multiuser Experimental Center) for the XPS and magnetization measurements, respectively. The authors also acknowledge Renato V. Gonçalves and Laécio Santos Cavalcante for the support.

## References

1. Corma, A.; Garcia, H.; *Chem. Soc. Rev.* **2008**, *37*, 2096.
2. della Pina, C.; Falletta, E.; Prati, L.; Rossi, M.; *Chem. Soc. Rev.* **2008**, *37*, 2077.
3. Giorgi, P. D.; Elizarov, N.; Antoniotti, S.; *ChemCatChem* **2017**, *9*, 1830.

4. Wang, D.; Villa, A.; Su, D.; Prati, L.; Schlögl, R.; *ChemCatChem* **2013**, *5*, 2717.
5. Ferraz, C. P.; Garcia, M. A. S.; Teixeira-Neto, É.; Rossi, L. M.; *RSC Adv.* **2016**, *6*, 25279.
6. Gualteros, J. A. D.; Garcia, M. A. S.; da Silva, A. G. M.; Rodrigues, T. S.; Cândido, E. G.; e Silva, F. A.; Fonseca, F. C.; Quiroz, J.; de Oliveira, D. C.; de Torresi, S. I. C.; de Moura, C. V. R.; Camargo, P. H. C.; de Moura, E. M.; *J. Mater. Sci.* **2019**, *54*, 238.
7. Olmos, C. M.; Chinchilla, L. E.; Villa, A.; Delgado, J. J.; Pan, H.; Hungría, A. B.; Blanco, G.; Clavino, J. J.; Prati, L.; Chen, X.; *Appl. Catal., A* **2015**, *525*, 145.
8. Long, N. Q.; Quan, N. A.; *React. Kinet., Mech. Catal.* **2015**, *114*, 147.
9. Prati, L.; Rossi, M.; *J. Catal.* **1998**, *176*, 552.
10. Prati, L.; Martra, G.; *Gold Bull.* **1999**, *32*, 96.
11. Porta, F.; Prati, L.; Rossi, M.; Coluccia, S.; Martra, G.; *Catal. Today* **2000**, *61*, 165.
12. Hashmi, A. S. K.; *Top. Organomet. Chem.* **2013**, *44*, 143.
13. Zhang, Y.; Yuwono, A. H.; Li, J.; Wang, J.; *Microporous Mesoporous Mater.* **2008**, *110*, 242.
14. Kumar, A.; Sreedhar, B.; Chary, K. V. R.; *J. Nanosci. Nanotechnol.* **2014**, *15*, 1714.
15. Wu, P.; Bai, P.; Yan, Z.; Zhao, G. X. S.; *Sci. Rep.* **2016**, *6*, 18817.
16. Corma, A.; Iborra, S.; *Adv. Catal.* **2006**, *49*, 239.
17. Carrettin, S.; McMorn, P.; Johnston, P.; Griffin, K.; Kiely, C. J.; Hutchings, G. J.; *Phys. Chem. Chem. Phys.* **2003**, *5*, 1329.
18. Zhang, G.; Hattori, H.; Tanabe, K.; *Appl. Catal.* **1988**, *36*, 189.
19. Costa, V. V.; Estrada, M.; Demidova, Y.; *J. Catal.* **2012**, *292*, 148.
20. de Moura, E. M.; Garcia, M. A. S.; Gonçalves, R. V.; Kiyohara, P. K.; Jardim, R. F.; Rossi, L. M.; *RSC Adv.* **2015**, *5*, 15035.
21. Dumbre, D. K.; Choudhary, V. R.; Patil, N. S.; Uphade, B. S.; Bhargava, S. K.; *J. Colloid Interface Sci.* **2013**, *415*, 111.
22. Estrada, M.; Costa, V. V.; Beloshapkin, S.; Fuentes, S.; Stoyanov, E.; Gusevskaya, E. V.; Simakov, A.; *Appl. Catal., A* **2014**, *473*, 96.
23. Castro, K. P. R.; Garcia, M. A. S.; de Abreu, W. C.; de Sousa, S. A. S.; de Moura, C. V. R.; Costa, J. C. S.; de Moura, E. M.; *Catalysts* **2018**, *8*, 83.
24. Rossi, L. M.; Garcia, M. A. S.; Vono, L. L. R.; *J. Braz. Chem. Soc.* **2012**, *23*, 1959.
25. Rossi, L. M.; Costa, N. J. S.; Silva, F. P.; Wojcieszak, R.; *Green Chem.* **2014**, *16*, 2906.
26. de Abreu, W. C.; Garcia, M. A. S.; Nicolodi, S.; de Moura, C. V. R.; de Moura, E. M.; *RSC Adv.* **2018**, *8*, 3903.
27. Kumar, A.; Kumar, V. P.; Kumar, B. P.; Vishwanathan, V.; Chary, K. V. R.; *Catal. Lett.* **2014**, *144*, 1450.
28. Ke, Y. H.; Qin, X. X.; Liu, C. L.; Yang, R. Z.; Dong, W. S.; *Catal. Sci. Technol.* **2014**, *4*, 3141.
29. Love, C. S.; Chechik, V.; Smith, D. K.; Wilson, K.; Ashworth, I.; Brannan, C.; *Chem. Commun.* **2005**, *15*, 1971.
30. <http://imagej.net>, accessed in February 2019.
31. *CasaXPS Processing Software*, version 2.3.15; Casa Software Ltd., Teignmouth, UK, 2018.
32. *ReX Powder Diffraction Analysis Software*, version 0.8.2; ReXpd Software Ltd., USA, 2016.
33. Crespo-Quesada, M.; Yarulin, A.; Jin, M.; Xia, Y.; Kiwi-Minsker; *J. Am. Chem. Soc.* **2011**, *133*, 12787.
34. Xia, Y.; Xiong, Y.; Lim, B.; Skrabalak, S. E.; *Angew. Chem., Int. Ed.* **2009**, *48*, 60.
35. Kudr, J.; Haddad, Y.; Richtera, L.; Heger, Z.; Cernak, M.; Adam, V.; Zitka, O.; *Nanomaterials* **2017**, *7*, 243.
36. Gao, L.; Wang, C.; Li, R.; Li, R.; Chen, Q.; *Nanoscale* **2016**, *8*, 8355.
37. Hu, L.; Zhang, R.; Chen, Q.; *Nanoscale* **2014**, *6*, 14064.
38. Yermakov, A. Y.; Feduschak, T. A.; Uimin, M. A.; Mysik, A. A.; Gaviko, V. S.; Chupakhin, O. N.; Shishmakov, A. B.; Kharchuk, V. G.; Petrov, L. A.; Kotov, Y. A.; *Solid State Ionics* **2004**, *172*, 317.
39. Nepak, D.; Srinivas, D.; *RSC Adv.* **2015**, *59*, 47740.
40. Mandal, S.; Santra, C.; Bando, K. K.; Jamesa, O. O.; Maity, S.; Mehta, D.; Chowdhury, B.; *J. Mol. Catal. A: Chem.* **2013**, *378*, 47.
41. Wang, W.; Fan, W.; He, Y.; Wang, J.; Kondo, J.; Tatsumi, T.; *J. Catal.* **2013**, *299*, 10.
42. Zhu, J.; Wang, P. C.; Lu, M.; *Appl. Catal., A* **2014**, *477*, 125.

Submitted: November 26, 2018

Published online: February 20, 2019

